



Article

Evaluating the generalization capability of MobileNet-based CNNs for temperature prediction in simulated specklegram fiber optic sensors with combined synthetic datasets and data augmentation

Isaac Huertas-Montes^{1,*}, Francisco Vélez^{2,3}, Víctor Aristizabal², Carlos Trujillo ³ and Jorge Herrera-Ramírez⁴

- Facultad de Ingenierías, Instituto Tecnológico Metropolitano, Medellín, Colombia.
- ² Facultad de Ingeniería. Universidad Cooperativa de Colombia, Medellín, Colombia.
- Escuela de Ciencias aplicadas e Ingeniería, Universidad EAFIT, Medellín, Colombia.
- Facultad de Ciencias Exactas y Aplicadas. Instituto Tecnológico Metropolitano, Medellín, Colombia.
- * Correspondence: johnhuertas250382@correo.itm.edu.co

Received: 01 December 2024; Accepted: 08 October 2025; Published: 21 October 2025

Abstract: The development of machine learning algorithms applied to specklegram-based sensors has facilitated the development of novel approaches for measuring several physical variables; however, most of these methods evaluate a single Fiber Specklegram Sensor (FSS) on a limited dataset. This paper assesses the generalization capability of applying these algorithms, in particular, Convolutional Neural Networks (CNN), to the prediction of temperature in simulated FSSs with different characteristics and conditions. This is achieved through the use of multiple combined synthetic datasets and data augmentation. The application of the Finite Element Method (FEM) enables the generation of datasets within the COMSOL Multi-physics software. The datasets are simulated with varying optical parameters, representing different optical fibers. Following the simulation of the datasets and training of selected models by combining them, data augmentation tests are conducted as though they were real fiber optic disturbances. Ultimately, a model is generated incorporating all the combined datasets and data augmentation, demonstrating the capacity of the model for generalization. This showcases the versatility of the computational methodology for evaluating, designing, and adjusting sensors without the need for experimental data. Additionally, it illustrates that a relatively simple model can be adapted to a variety of sensing system scenarios and configurations.

© 2025 by the authors. Published by Universidad Tecnológica de Bolívar under the terms of the Creative Commons Attribution 4.0 License. Further distribution of this work must maintain attribution to the author(s) and the published article's title, journal citation, and DOI. https://doi.org/10.32397/tesea.vol6.n2.802

How to cite this article: Huertas-Montes, Isaac; Vélez, Francisco; Aristizabal, Víctor; Herrera-Ramirez, Jorge; Trujillo, Carlos. Evaluating the generalization capability of MobileNet-based CNNs for temperature prediction in simulated specklegram fiber optic sensors with combined synthetic datasets and data augmentation. *Transactions on Energy Systems and Engineering Applications*, 6(2): 802, 2025. DOI:10.32397/tesea.vol6.n2.802

Trans. Energy Syst. Eng. Appl., 6(2): 802, 2025

1. Introduction

Fiber optic sensors can discern various characteristics of optical light signals, such as phase, intensity, and polarization. These signals are sensitive to physical changes in the fiber and allow the identification of such variations [1], including those related to temperature, pressure, bending, twisting, refractive index, and vibration [1–3]. Fiber-optic speckle sensors combine high sensitivity with distributed sensing along the fiber [4] and intrinsic immunity to electromagnetic interference [5], features that are valuable in industrial process control and harsh-environment monitoring. Because the speckle pattern varies predictably with temperature, a properly calibrated system can provide accurate, spatially resolved temperature measurements. Reliable deployment, therefore, requires distinguishing temperature-induced speckle variations from those produced by strain, vibration, or other environmental factors, and this is now being achieved by using machine learning approaches [6]. The optical modal interference patterns called speckle or specklegrams are formed from the optical trajectories generated by the different propagation modes, these can be simulated by numerical modeling techniques such as the Finite Element Method (FEM) [7,8] or Finite Difference Method [9], which allow the representation and analysis of the propagation phenomenon in optical fibers and the generation of synthesized speckle patterns. Fiber specklegram sensors (FSS) measure fiber disturbances by focusing specifically on the speckle generated by the optical fiber, and have shown significant potential in industrial applications. These applications include the detection of fiber bending in mining environments [10], structural monitoring [11], multi-joint bending sensing [12], image reconstruction, development of fiber optic-based tactile sensors [13], and prediction of surface friction characteristics [14]. In the medical field it is also possible to find applications involving the analysis of optical signals resulting from disturbances in the optical fiber, as is the case of biosensors for antigens such as CEACAM5 [15], or fiber optic applications for patient monitoring [16, 17]. This illustrates the remarkable versatility and adaptability of these sensors.

Traditional signal-processing methods, most notably cross-correlation, have long been used to analyze the spatial evolution of speckle patterns and to infer perturbations along the fiber [18, 19]. While effective in controlled settings, these techniques depend on hand-crafted similarity metrics and are sensitive to environmental noise. The recent adoption of machine-learning strategies, especially convolutional neural networks (CNNs), has enabled data-driven feature extraction that is better suited to the high dimensionality and non-linear behaviour of fiber specklegrams [20–24]. CNNs not only attenuate noise originating from external disturbances [25], but also extend the dynamic range and enhance the sensitivity of fibre-specklegram sensors [26]. These developments have notably expanded the functionality and potential applications of fiber speckle sensing (FSS) systems.

Investigations in the field of FSS have utilized both synthetic and real-world datasets. Synthetic data offer the advantage of examining a wide variety of system parameters under controlled conditions [27,28]. Conversely, experimental data provide real-world validation but require considerable time, resources, and manual effort for acquisition, particularly when performed without automation [6, 22–24]. Given the importance of large datasets for training machine learning models and the limited size of typical experimental datasets, we focus on physics-based simulations and combine several synthetic datasets under varied operating conditions.

This study focuses on the evaluation of the generalization capability of a machine learning model with the MobileNet architecture for FSS for temperature prediction. Several models trained on up to three synthetic datasets of specklegrams simulated by the Finite Element Method (FEM) were compared. Each dataset belongs to an optical fiber with different optical parameters such as wavelength, numerical aperture, core diameter, and cladding diameter. It was proposed to test the ability of the neural network to obtain accurate and precise temperature data.

In addition, data augmentation is proposed to evaluate its effectiveness and assess the necessity of having a larger dataset for this type of application. Five geometric transformations were applied to the speckle images: zoom, sharp, rotation and noise changes.

The manuscript is organized as follows: the method (Section 2) describes the simulation of specklegrams using the Finite Element Method (FEM), the characteristics of the synthetic datasets used, the MobileNet-based CNN architecture, and the data augmentation techniques applied. Section 3 presents the results and discussion, focusing on model performance metrics and how different data augmentation strategies affect model accuracy. Section 4 summarizes the key findings, highlighting the model's ability to generalize across different sensor configurations using synthetic data and controlled data augmentation. Finally, acknowledgments, references, and author contributions are provided at the end of the manuscript.

2. Methods

2.1. Specklegram Simulation

Synthetic specklegram simulations were performed using the Finite Element Method (FEM) within COMSOL Multiphysics, integrated with Matlab. This model simulated the propagation of an optical field through a multimode optical fiber, concentrating specifically on the sensing region affected by temperature fluctuations. This method facilitated an accurate approximation of the behavior of the fiber under perturbations, excluding undisturbed regions to optimize computational efficiency [26].

Through this FEM model, the vector wave Equation 1 was numerically solved for each propagation mode within the multimode optical fiber (MMF) under analysis [26, 29].

$$\nabla \times \nabla \times \vec{E} - k_0^2 n^2 \vec{E} = 0 \tag{1}$$

Here \vec{E} , represents the electric field of each mode, k_0 is the wavenumber in vacuum, and n stands for the refractive index of the MMF. The refractive index can further be updated in response to thermal fluctuations using Equation 2.

$$n \approx n_0 + C_{T0}(T - T_0) \tag{2}$$

Where C_{TO} is the thermo-optic coefficient, n_0 the reference index, T_0 the reference temperature, and T the temperature to be measured. The initial core refractive index is calculated using the Sellmeier equation [26], while the cladding refractive index n_{0cla} is given by Equation 3.

$$n_{0cla} = \sqrt{n_{0co}^2 - NA^2} \tag{3}$$

Where n_0co is the initial core refractive index and NA is the numerical aperture.

2.2. Computational Cost of the Specklegram simulations

The COMSOL Multiphysics simulation employs the Wave Optics Module with a 2.5D beam-envelope formulation. This approach reduces computational complexity by focusing on the 2D fiber cross-section rather than the full 3D geometry, making the computational load proportional to the cross-sectional mesh density rather than fiber length. The simulation solves for the slowly varying electric field envelope of each propagating mode, maintaining approximately 2×10^5 degrees of freedom (DOF) using $\sim 64 \times 10^3$ second-order triangular elements. On a consumer-grade system (AMD Ryzen 5 4500, 32 GB RAM), processing a 126×126-pixel specklegram requires approximately 50 seconds of total computation time, including meshing, assembly, solving, and sampling. The computational efficiency stems from two key

factors: the linear scaling properties of the iterative solver with respect to DOF, and the dimensionality reduction inherent in the 2.5D formulation [30]. In comparison, an equivalent full 3D vector finite element model would increase the DOF by approximately one order of magnitude, escalating memory requirements to multi-gigabyte levels and extending solve times proportionally [31].

2.3. Dataset Characteristics

Then, using the FEM method, three data sets were synthesized: two, named DI and DIII, with a temperature range of 0°C to 100°C in steps of 0.1°C; and the other, named DII, from 0°C to 120°C in steps of 0.2°C. The DI and DIII data sets have mostly similar optical parameters except for the numerical aperture (NA), which is 0.13 and 0.3, respectively. The DII dataset has a numerical aperture of 0.22, but it also differs from the other two datasets for all optical parameters. This difference can be seen in Table 1.

Dataset	DI	DII	DIII
Numerical aperture (nm)	0.13	0.22	0.3
Wavelength (nm)	632.8	1490	632.8
Core Diameter (µm)	9	50	9
Cladding Diameter (µm)	40	125	40
Core Index	1.457	1.4447	1.448
Cladding Index	1.4521	1.4279	1.4166
length of the Perturbation (mm)	0.3	2.5	0.3

Table 1. Optical parameters for the FEM simulation.

By employing the aforementioned optical parameters and the finite element method (FEM), specklegrams similar to those illustrated in Figure 1 are generated, exhibiting one for each dataset at 50 °C. These images illustrate the impact of varying the numerical aperture in the simulations.

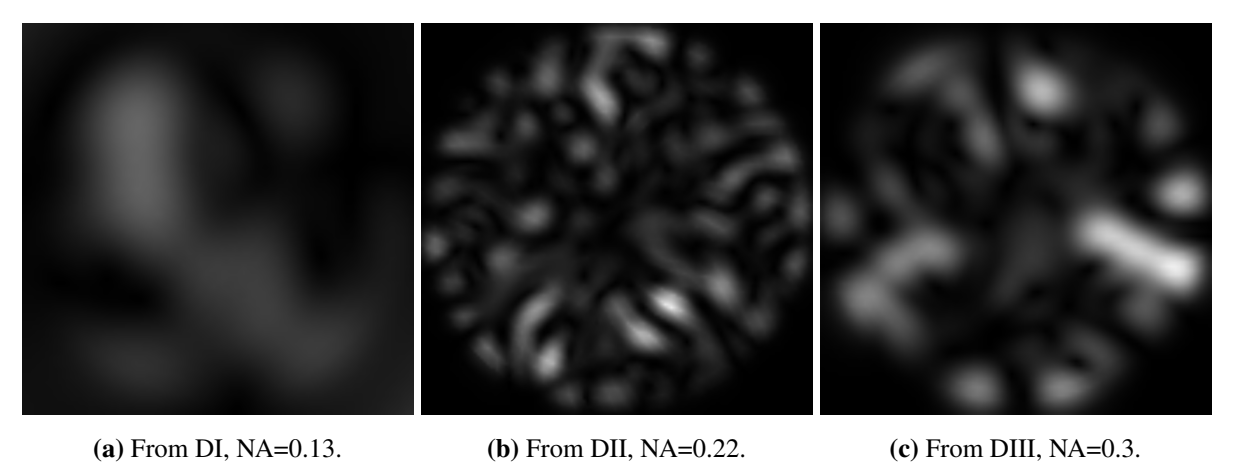


Figure 1. Simulated fiber optic specklegrams at 50°C.

From these datasets, four models were trained, each with different combinations of the datasets. Table 2 shows how these datasets were combined and how the models were nominated.

For all tests performed in this study, the data were split as follows: 70% training, 20% validation, and 10% testing.

2.4. Convolutional Neural Network Architecture

MobileNet architecture (MNet), which is designed as a classification algorithm, is used as the base architecture to train these models. The architecture is loaded with weights that have been pre-trained

Model	Alpha	Beta	Gamma	Delta
Dataset	DII	DI and DII	DII and DIII	DI, DII and DIII
Temperature Range(<i>C</i>)	0 to 120	0 to 100	0 to 120	0 to 100
Number of images	601	1003	1203	1504

Table 2. Datasets used on the CNN models trained.

using the ImageNet database. Since we are sensing temperature, which is a continuous variable, a transfer learning technique was performed at the output of this architecture, adding dense layers and a single artificial neuron at the output with a linear activation function for regression. The hyperparameters used in this study for this architectural configuration, as shown in Figure 2, are 50 epochs, 10 trainable layers in the MobileNet architecture, and a learning rate of 1.17×10^{-4} , as these parameters demonstrated optimal performance in the training process. As mentioned before, at the output of the MobileNet architecture two dense layers with ReLu activation function and 1024 artificial neurons were added, followed by an output layer with a Linear activation function and a single neuron, in order to transform this classification architecture into a regression architecture.

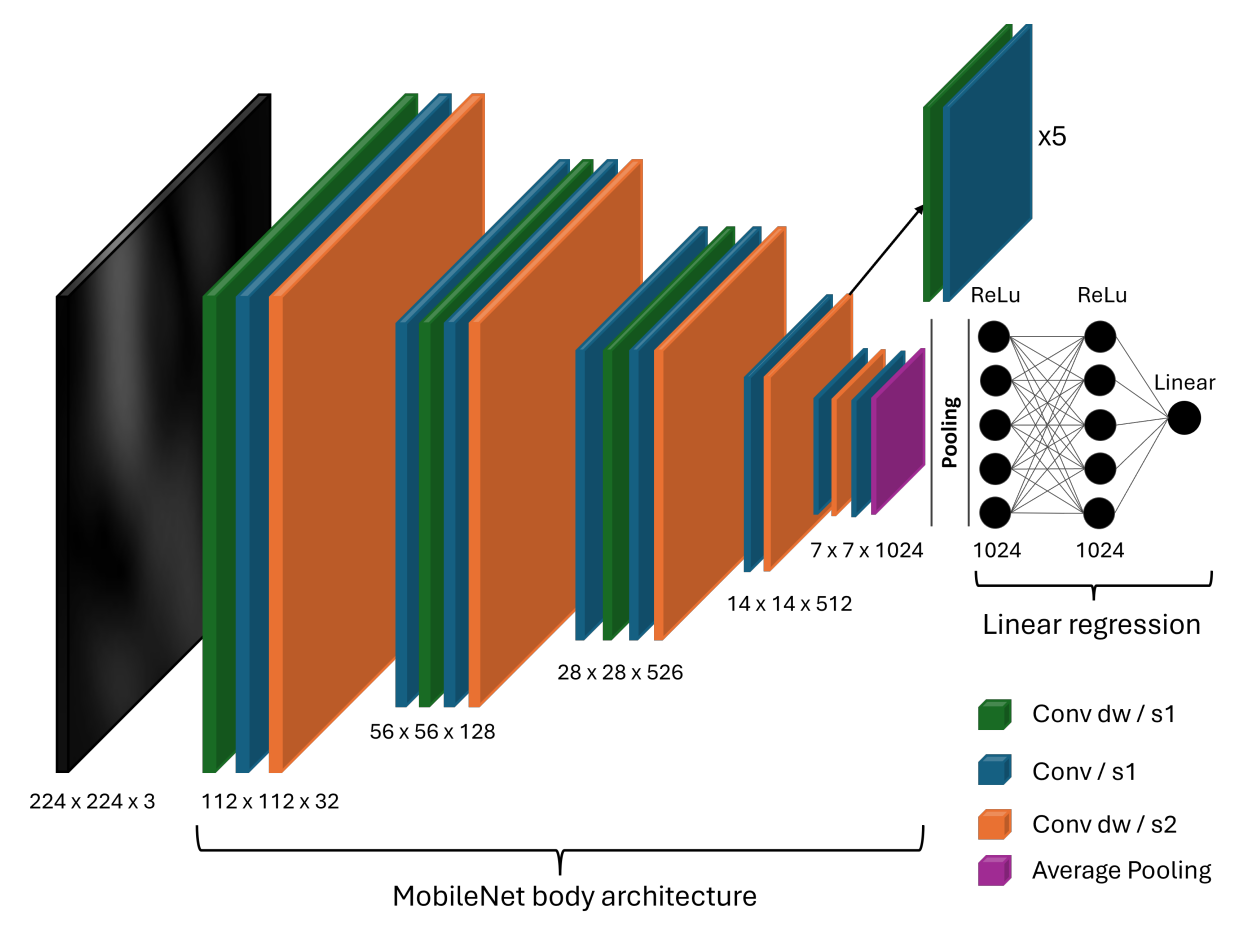


Figure 2. MobileNet architecture transformed into a regression architecture.

2.5. Data Augmentation

After testing the ability of the models to generalize the datasets, data augmentation tests were conducted. Table 3 lists the transformations and parameters to which they were applied. All tests were performed with random values within the ranges listed in Table 3. Transformations were performed sequentially on the same images. Initially, image augmentation was tested using only the DII dataset.

Table 3. Limits of image transformation factors.

Rotation	0° to 360°
Zoom	95% to 105%
Shift	0% to 0.8%
Noise	0% to 5% standard deviation

First, data augmentation is performed on all successive transformations, and to reduce the model error, each transformation is tested individually, and the transformation with the greatest impact on the model error is identified. Finally, we eliminated the transformation with the highest error to test the usefulness of data augmentation in this type of situation.

Using the transformations resulting from the debugging of those that most affect the error, we increase the data of the three datasets for the Delta model and finally validate the generalization capacity of the model with datasets whose optical parameters are very diverse, in addition to the large amount of added data.

3. Results and Discussion

The initial model outcomes were derived from the analysis of various combinations of data sets, as previously described. To evaluate and demonstrate the performance of the models, several metrics were calculated, including mean squared error (MSE), root mean squared error (RMSE), mean absolute error (MAE), maximum error (MAXE) and R^2 . The results are presented in Table 4. These metrics are considered to provide a comprehensive evaluation of CNN models. MSE and RMSE quantify the average prediction error, with a greater emphasis on larger deviations, while MAE offers a less skewed measure of the average error magnitude. MAXE is crucial for identifying the worst-case prediction error, vital for sensor reliability. Finally, R^2 assesses the model's overall goodness of fit and its ability to explain the variance in the temperature data.

Table 4. Performance metrics for each model.

Model	$MSE ({}^{\circ}C^2)$	RMSE (℃)	MAE (℃)	MAXE (℃)	R^2 score
Alpha	2.00	1.41	1.17	3.14	0.998358
Beta	7.24	2.69	2.10	11.49	0.990882
Gamma	0.60	0.78	0.63	1.93	0.999458
Delta	2.40	1.55	0.98	10.47	0.996972
VGG-Reg [21]	2.00	1.42	1.31	2.85	0.998000
Correlation coefficient [21]	10.30	3.21	2.45	9.08	0.992000

Table 4 reveals the ability of the model to determine the temperature from speckle patterns despite training on datasets with significantly different optical parameters. The model not only exhibits a high degree of fit, but also shows improvement in certain metrics. This is evidenced by the MSE of the Gamma model, which is approximately three times lower than that of the Alpha model (Gamma MSE = 0.6 compared to Alpha MSE = 2). The dataset used to train this Alpha model (dataset DII) was also used in a

previous work where an architecture with a VGG structure (conv > RELU > conv-RELU > MaxPooling blocks) produced similar results, also a correlation coefficient method was carried out and this results were compared [21], as shown in Table 4. In contrast, when multiple datasets are combined for training, the performances are variable, but the Gamma model that includes the datasets DII and DIII shows improvement in all metrics, surpassing all others.

Following testing of the capacity of the model to generalize across datasets with varying optical parameters, the efficacy of data augmentation was evaluated. Initially, the Alpha dataset was augmented, as follows: First, all the previously mentioned transformations were applied consecutively, and each transformation was applied independently. Finally, after identifying the transformation that contributes the most to the error, data augmentation is performed again with all the transformations except the one that contributed to the higher error. Table 5 lists the error results for each test.

Model	MSE (°C2)	RMSE (°C)	MAE (°C)	MAXE (°C)	R ² score
Alpha_All	103.09	10.15	8.41	32.66	0.915162
Alpha_Rotation	26.38	5.14	4.25	15.37	0.978288
Alpha_Zoom	2.29	1.51	1.14	4.41	0.998114
Alpha_Shift	1.53	1.24	1.04	2.72	0.998741
Alpha_Noise	3.71	1.93	1.57	4.96	0.996950
Alpha _All/R	12.90	3.59	3.05	10.30	0.989385

Table 5. Performance metrics for augmented data for Alpha model.

As shown in Table 5, the rotation in an arbritrary orientation exhibits a considerable degree of inaccuracy with regard to the other transformation. Consequently, it is excluded from the data augmentation process and is currently applied solely in conjunction with the remaining four transformations. As a result, the model demonstrated enhanced accuracy.

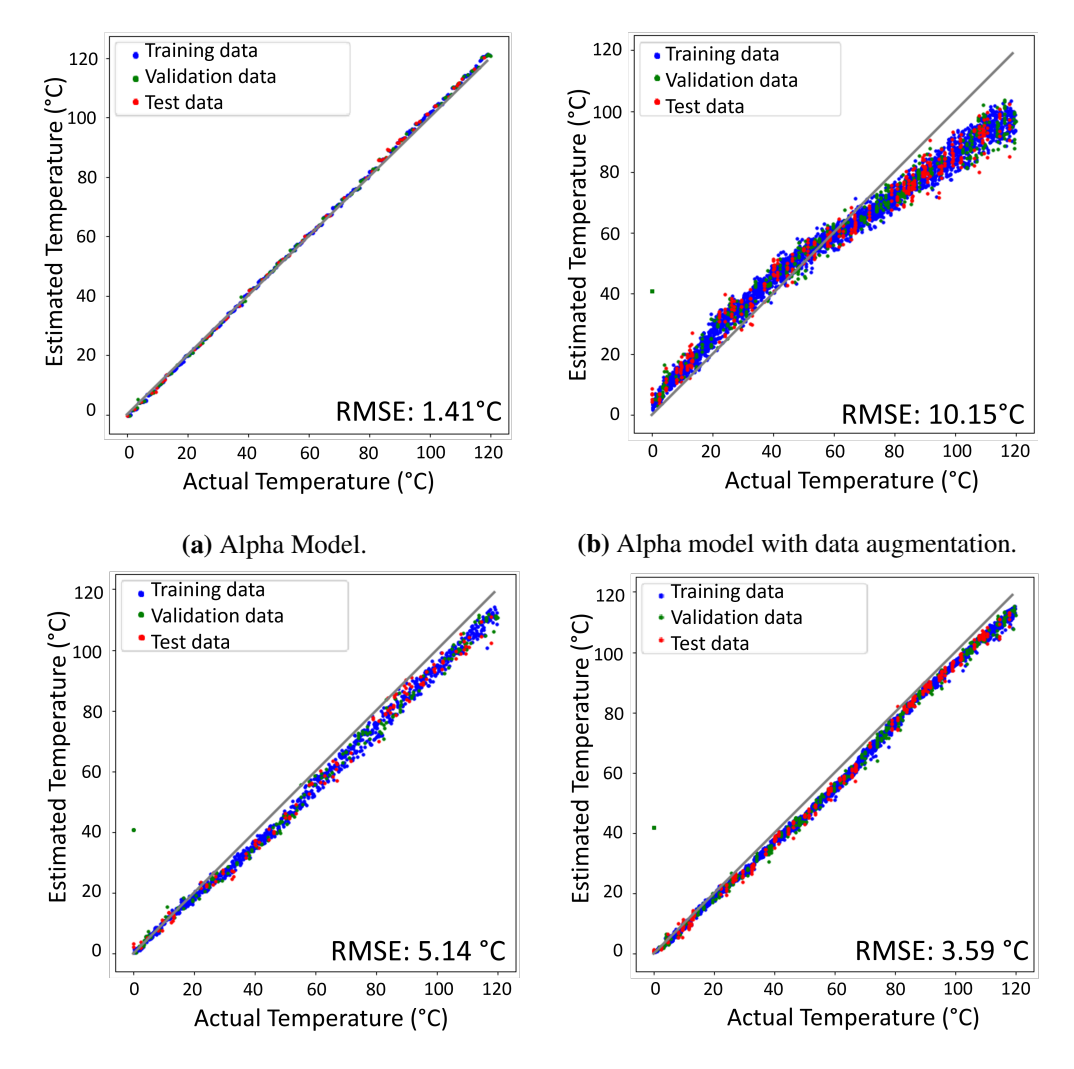
Figure 3 illustrates the efficacy of the data augmentation in the model. In the figures, the actual temperature is considered as the temperature indicated by the simulation. Figure 3a depicts the Alpha model without any data augmentation, and the metrics are shown in Table 4. Figure 3b illustrates the performance of the Alpha model with augmented data and all the transformation mentioned. Figure 3c depicts the Alpha model augmented only with rotation. Figure 3d depicts the performance of the Alpha model with all transformations for data augmentation, with the exception of rotation.

Rotation tests were subsequently conducted with constrained angular displacement to determine the optimal maximum angle that most accurately simulated real FSS conditions while maximizing the model precision. Table 6 lists the data augmentation metrics for a restricted rotation angle from 5 to 60 degrees.

Max angle (°)	$MSE(C^2)$	RMSE (C)	MAE(C)	MAXE(C)	R ² score
5	1.11	0.83	1.05	3.48	0.998769
10	1.06	0.81	1.03	3.66	0.998788
15	1.83	1.03	1.35	6.33	0.997906
30	3.01	1.05	1.73	31.67	0.996562
45	3.40	1.23	1.84	26.78	0.995779
60	6.69	1.50	2.59	38.08	0.991791

Table 6. Metrics of limited rotation transformation for Delta model.

Table 6 shows an inversely proportional relationship between the maximum angle of rotation and accuracy of the Delta model. Therefore, it is proposed for future work to incorporate angle-limited rotation into the data enhancement, taking into account the possible rotation of the speckle in real FSS applications.



- (c) Alpha model with only rotation as data augmentation.
- **(d)** Alpha model with all transformations except rotation.

Figure 3. Graphs of actual vs. estimated temperatures in the range of 0°C to 120°C for the different models described above.

Following the demonstration of the efficacy of limited data augmentation in the Alpha model, the Delta model has been subjected to the same process. Table 7 illustrates the resulting metrics when training this model with all transformations, with the exception of rotation.

Table 7. Comparison of delta model metrics with and without data augmentation.

Model	$MSE(C^2)$	RMSE(C)	MAE(C)	MAXE(C)	R ² score
Delta	2.40	1.55	0.98	10.47	0.996972
Delta Aum	1.64	1.28	0.97	5.22	0.998039

The efficacy of data augmentation was validated by the information presented in Table 7 and Figure 4. However, this evaluation was conducted without the rotations that can commonly appear in real fiber optic applications. To avoid the elimination of rotation during data augmentation, its inclusion is considered

but in a delimited range. This could pave the way for its integration into the data augmentation process, alongside other transformations.

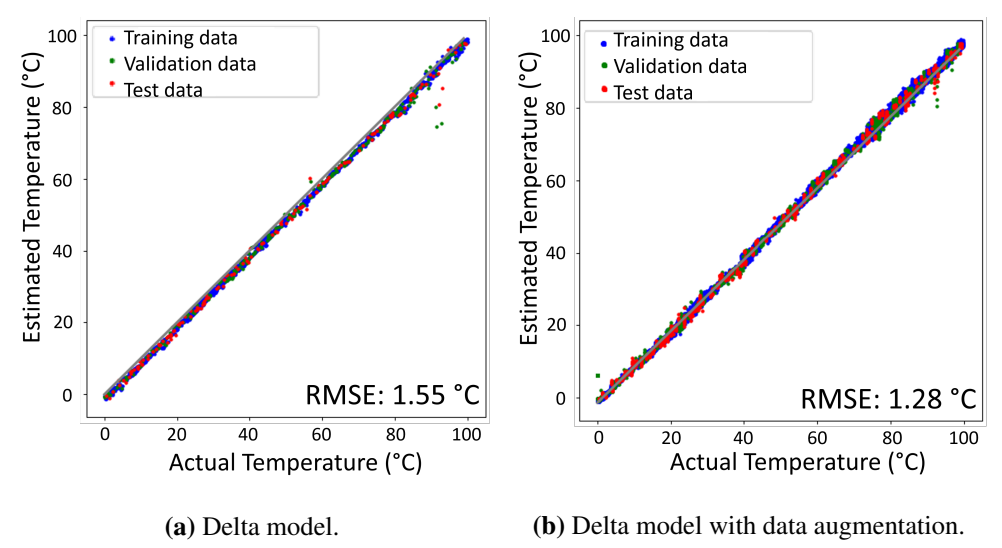


Figure 4. Comparison of actual and estimated temperatures for the Delta model with and without data augmentation.

Arbitrary rotation negatively impacts the model because speckle patterns are highly sensitive to orientation, disrupting the spatial features the CNN learns to associate with temperature. This leads to increased data variability that is not directly correlated with temperature. However, since the performance degradation was around 2% (decrease in R² from 0.998358 to 0.978288)and could be reduced by limiting the range of rotation during data augmentation to more physically plausible scenarios, controlling the rotation range during training is a key mitigation strategy.

4. Conclusions

Machine learning models are highly effective at performing image and pattern recognition. They can generalize between data sets derived from simulations with different parameters, although their impact on the generated images is minimal. This was observed in the Alpha model, which is a set of images very similar to the one in Figure 1b. Despite the lack of noticeable change between images when changing 0.1°C , the model achieved a high degree of recognition.

From simulated datasets, satisfactory results are obtained in Table 4, where it is noted that all all trained models achieved an R^2 score exceeding 0.99. Among them, the gamma model, trained with datasets DII and DIII, demonstrated the best performance, achieving a root mean squared error (RMSE) of 0.78 °C, nearly halving the error of the alpha model, which exhibited an RMSE of 1.41 °C.

The results of data augmentation reveal a notable initial root mean square error (RMSE) of 10.15 °C for the alpha model enhanced with all transformations, approximately seven times larger than the error of the model without augmented data (1.41 °C). However, limiting the data augmentation by excluding the rotation transformation, which alone resulted in an RMSE of 5.14 °C, improves the final alpha model to an RMSE of 3.59 °C, significantly outperforming the model augmented with the rotation included.

Limiting the rotation angle in data augmentation shows a clear improvement, with a maximum angle of 10° providing the best accuracy without compromising model performance.

These results demonstrate the model's ability to generalize across different FSS, making it adaptable to a wider range of conditions without the need for retraining on specific sensor configurations.

Future investigations will focus on enhancing the predictive capacity and robustness of these models by integrating synthetic datasets with experimental ones. This combination could bridge the gap between simulation and real-world application, potentially leading to more accurate and reliable sensor readings. Furthermore, incorporating additional physical variables, such as strain and curvature, into the simulations and analyses would allow for a more comprehensive assessment of the sensor's mechanical performance alongside its temperature sensing capabilities, paving the way for multi-parameter FSS development.

Acknowledgments

Funding: This work was partially funded by Universidad Cooperativa de Colombia (UCC) (INV3612); Instituto Tecnológico Metropolitano (ITM) (PE24201), EAFIT University and MINCIENCIAS National Doctorates program.

Author contributions: Conceptualization, J. H. and F.V.; Methodology, J.H., F.V. C.T. and V.A; Software, V.A., F.V. and I.H.; Validation, I.H., J.H and F.V.; Formal Analysis, J.H., C.T. and F.V.; Investigation, I.H., J.H. and F.V.; Writing – Original Draft Preparation, I.H.; Writing – Review & Editing, J.H., C.T. and F.V.; Supervision, J.H. and F. V.

Disclosure statement: The authors declare that they have no financial, personal, or professional conflicts of interest that could influence the results or interpretation of this research.

References

- [1] Jianli Liu, Yuxin Ke, Dong Yang, Qiao Deng, Chuang Hei, Hu Han, Daicheng Peng, Fangqing Wen, Ankang Feng, and Xueran Zhao. Deep learning-based simultaneous temperature- and curvature-sensitive scatterplot recognition. *Sensors*, 24(13), 2024.
- [2] Mohammad Istiaque Reja, Darcy L. Smith, Linh Viet Nguyen, Heike Ebendorff-Heidepriem, and Stephen C. Warren-Smith. Multimode optical fiber specklegram pressure sensor using deep learning. *IEEE Transactions on Instrumentation and Measurement*, 73:1–10, 2024.
- [3] Ivan Chapalo, Andreas Stylianou, Patrice Mégret, and Antreas Theodosiou. Advances in optical fiber speckle sensing: A comprehensive review. *Photonics*, 11(4), 2024.
- [4] Shichao Yue, Huizhen Lu, Boyi Li, and Zifan Che. Feasibility of a specklegram-based quasi-distributed temperature sensor with principal component analysis and variational autoencoder. *IEEE Sensors Journal*, 24(14):22410–22418, 2024.
- [5] Fang Zhao, Weihao Lin, Penglai Guo, Jie Hu, Yuhui Liu, Shuaiqi Liu, Feihong Yu, Guomeng Zuo, Guoqing Wang, Huanhuan Liu, Jinna Chen, Yi Li, Perry Ping Shum, and Liyang Shao. Compact optical fiber sensor based on vernier effect with speckle patterns. *Opt. Express*, 31(22):36940–36951, Oct 2023.
- [6] Hanchao Sun, Jixuan Wu, Binbin Song, Binbin Song, Jifang Wang, and Xiao Liu. Speckle-decoded temperature-insensitive strain identification in a multimode optical fiber. *Optics Letters, Vol. 49, Issue 21, pp. 6185-6188*, 49:6185–6188, 11 2024.
- [7] V. H. Arístizabal, F. J. Vélez, E. Rueda, N. D. Gómez, and J. A. Gómez. Numerical modeling of fiber specklegram sensors by using finite element method (fem). *Opt. Express*, 24(24):27225–27238, Nov 2016.
- [8] Juan Arango, Victor Aristizabal, Francisco Vélez, Juan Carrasquilla, Jorge Gomez, Jairo Quijano, and Jorge Herrera-Ramirez. Synthetic dataset of speckle images for fiber optic temperature sensor. *Data in Brief*, 48:109134, 2023.

- [9] Madhu Veettikazhy, Anders Kragh Hansen, Dominik Marti, Stefan Mark Jensen, Anja Lykke Borre, Esben Ravn Andresen, Kishan Dholakia, and Peter Eskil Andersen. Bpm-matlab: an open-source optical propagation simulation tool in matlab. Opt. Express, 29(8):11819–11832, Apr 2021.
- [10] Brian Pamukti, Zi Wang, Muhammad Fajar Faliasthiunus Pradipta, Shien-Kuei Liaw, Chien-Hung Yeh, and Fu-Liang Yang. Deep learning and time series signal processing for bending detection in mining environment using optical fiber sensor. Optical Fiber Technology, 88:103819, 2024.
- [11] Juan Sanguino-Lemus, Gustavo Hernández-Martínez, and Carla Puerto-López. Monitoreo estructural basado en sistemas de sensores de fibra óptica. *Revista de Ingenierías Interfaces*, 3:73–97, 2020.
- [12] Guangde Li, Yan Liu, Lezhi Pang, Hui Yuan, and Muguang Wang. A novel structure with ultra short multimode fiber for fiber specklegram sensor and its application in multi-bending sensing. proof and concept. *Journal of Lightwave Technology*, pages 1–9, 2024.
- [13] Asif Newaz, Md Omar Faruque, Rabiul Al Mahmud, Rakibul Hasan Sagor, and Mohammed Zahed Mustafa Khan. Machine-learning-enabled multimode fiber specklegram sensors: A review. *IEEE Sensors Journal*, 23(18):20937–20950, 2023.
- [14] Wataru Matsuda, Yuji Yuhara, Kaisei Sato, and Shinya Sasaki. A study on prediction of friction characteristics from speckle patterns of friction surfaces using machine learning. *Tribology Online*, 19(4):334–344, 2024.
- [15] Yuhui Liu, Weihao Lin, Fang Zhao, Yibin Liu, Junhui Sun, Jie Hu, Jialong Li, Jinna Chen, Xuming Zhang, Mang I. Vai, Perry Ping Shum, and Liyang Shao. A multimode microfiber specklegram biosensor for measurement of ceacam5 through ai diagnosis. *Biosensors*, 14(1), 2024.
- [16] Alberto Rodríguez-Cuevas, Eusebio Real Pena, Luis Rodríguez-Cobo, Mauro Lomer, and José Miguel López-Higuera. Low-cost fiber specklegram sensor for noncontact continuous patient monitoring. *Journal of Biomedical Optics*, 22(3):037001, 2017.
- [17] Laura Susana Vargas-Valencia, Felipe B. A. Schneider, Arnaldo G. Leal-Junior, Pablo Caicedo-Rodríguez, Wilson A. Sierra-Arévalo, Luis E. Rodríguez-Cheu, Teodiano Bastos-Filho, and Anselmo Frizera-Neto. Sleeve for knee angle monitoring: An imu-pof sensor fusion system. *IEEE Journal of Biomedical and Health Informatics*, 25(2):465–474, 2021.
- [18] Eric Fujiwara, Murilo Ferreira Marques dos Santos, and Carlos Kenichi Suzuki. Optical fiber specklegram sensor analysis by speckle pattern division. *Applied Optics*, 56:1585, 2 2017.
- [19] Fedor Gubarev, Lin Li, Miron Klenovskii, and Anatoliy Glotov. Speckle pattern processing by digital image correlation. *MATEC Web of Conferences*, 48:04003, 4 2016.
- [20] Yan Liu, Guangde Li, Qi Qin, Zhongwei Tan, Muguang Wang, and Fengping Yan. Bending recognition based on the analysis of fiber specklegrams using deep learning. *Optics Laser Technology*, 131:106424, 11 2020.
- [21] Francisco Velez Hoyos, Juan David Arango Moreno, Victor Aristizabal, Carlos Trujillo, and Jorge Herrera Ramirez. Comparative performance evaluation of classical methods and a deep learning approach for temperature prediction in fiber optic specklegram sensors. *Computer Optics*, 48:689–695, 09 2024.
- [22] Xinliang Gao, Jixuan Wu, Binbin Song, Haifeng Liu, Shaoxiang Duan, Zhuo Zhang, Xiao Liu, and Hanchao Sun. Deep learning for temperature sensing with microstructure fiber in noise perturbation environment. *IEEE Photonics Technology Letters*, 35:1247–1250, 12 2023.
- [23] Darcy L. Smith, Linh V. Nguyen, David J. Ottaway, Thiago D. Cabral, Thiago D. Cabral, Eric Fujiwara, Cristiano M. B. Cordeiro, Cristiano M. B. Cordeiro, Stephen C. Warren-Smith, Stephen C. Warren-Smith, and Stephen C. Warren-Smith. Machine learning for sensing with a multimode exposed core fiber specklegram sensor. *Optics Express, Vol. 30, Issue 7, pp. 10443-10455*, 30:10443–10455, 3 2022.
- [24] Guangde Li, Yan Liu, Qi Qin, Xiaoli Zou, Muguang Wang, and Fengping Yan. Deep learning based optical curvature sensor through specklegram detection of multimode fiber. *Optics Laser Technology*, 149:107873, 5 2022.

- [25] Fu Feng, Jiaan Gan, PengFei Chen, Wei Lin, Guang Yong Chen, Changjun Min, Xiaocong Yuan, and Michael Somekh. Ai-assisted spectrometer based on multi-mode optical fiber speckle patterns. *Optics Communications*, 522:128675, 2022.
- [26] Juan David Arango Moreno, Yeraldin Velez, Victor Aristizabal, Francisco Velez, Gómez Alberto, Jairo Quijano, and Jorge Herrera Ramirez. Numerical study using finite element method for the thermal response of fiber specklegram sensors with changes in the length of the sensing zone. *Computer Optics*, 45:534–540, 07 2021.
- [27] Juan Arango, Victor Aristizabal, Francisco Vélez, Juan Carrasquilla, Jorge Gomez, Jairo Quijano, and Jorge Herrera-Ramirez. Synthetic dataset of speckle images for fiber optic temperature sensor. *Data in Brief*, 48:109134, 6 2023.
- [28] Francisco J. Vélez, Juan D. Arango, Víctor H. Aristizábal, Carlos Trujillo, and Jorge A. Herrera-Ramírez. Experimental dataset for fiber optic specklegram sensing under thermal conditions and use in a deep learning interrogation scheme. *Data*, 10:44, 3 2025.
- [29] Luis Castaño, Luis Gutierrez, Jairo Quijano, Jorge Herrera-Ramírez, Alejandro Hoyos, Francisco Vélez, Víctor Aristizabal, Luiz Silva-Nunez, and Jorge Gómez. Temperature measurement by means of fiber specklegram sensors (fss). *Óptica Pura y Aplicada*, 2018.
- [30] Walter Frei. How large of a model can you solve with comsol®? COMSOL Blog, 2022.
- [31] COMSOL. How to estimate the number of degrees of freedom in a model. COMSOL Learning Center, 2023.